

# Model-Augmented Nearest-Neighbor Estimation of Conditional Mutual Information for Feature Selection

Alan Yang\*, AmirEmad Ghassami\*, Maxim Raginsky\*, Negar Kiyavash<sup>†</sup>, and Elyse Rosenbaum\*

\*Department of Electrical and Computer Engineering, University of Illinois at Urbana-Champaign, Urbana, IL 61801, USA

<sup>†</sup>College of Management of Technology, École Polytechnique Fédérale de Lausanne (EPFL), Switzerland

Email: asyang2@illinois.edu, ghassam2@illinois.edu, maxim@illinois.edu, negar.kiyavash@epfl.ch, elyse@illinois.edu

**Abstract**—Markov blanket feature selection, while theoretically optimal, generally is challenging to implement. This is due to the shortcomings of existing approaches to conditional independence (CI) testing, which tend to struggle either with the curse of dimensionality or computational complexity. We propose a novel two-step approach which facilitates Markov blanket feature selection in high dimensions. First, neural networks are used to map features to low-dimensional representations. In the second step, CI testing is performed by applying the  $k$ -NN conditional mutual information estimator to the learned feature maps. The mappings are designed to ensure that mapped samples both preserve information and share similar information about the target variable if and only if they are close in Euclidean distance. We show that these properties boost the performance of the  $k$ -NN estimator in the second step. The performance of the proposed method is evaluated on synthetic, as well as real data pertaining to datacenter hard disk drive failures.

## I. INTRODUCTION

A prominent approach for selecting features relevant to a target variable is to choose a minimal set that renders the target variable conditionally independent of the rest of the features. This approach is referred to as Markov blanket feature selection, and has attracted wide attention due to its theoretical optimality and strong performance [Aliferis et al., 2010].

However, testing for conditional independence (CI) from data is a notoriously challenging task, especially for continuous-valued variables [Paninski, 2003]. In this setting, one of the most promising approaches is based on  $k$ -nearest neighbor ( $k$ -NN) estimation of the conditional mutual information (CMI) [Runge, 2018], an information-theoretic measure capable of capturing nonlinear relationships.

The  $k$ -NN method is fast and reliable for many applications. Unfortunately,  $k$ -NN suffers from the curse of dimensionality [Gao et al., 2018]. As shown in Section IV, this problem is further exacerbated when dealing with data for which the Euclidean distance is a weak measure of similarity (e.g., in time-series). Alternatively, kernel-based methods are known for their ability to handle high dimensions, but scale poorly with sample size since large kernel matrices need to be computed [Fukumizu et al., 2004]. Due to these limitations, CI testing and Markov blanket identification in the continuous case have largely been limited to the low- to moderate-dimensional case.

Several model-based approaches have been proposed to handle mutual information estimation [Belghazi et al., 2018] and CI testing [Sen et al., 2017] in high dimensions. These methods leverage the representational power of neural networks to model complex relationships between variables, and have demonstrated state-of-the-art performance for their respective tasks. While powerful, model-based methods require an individual neural network to be trained and tuned for each CI test performed, and are therefore computationally infeasible for Markov blanket feature selection, where the number of required CI tests can be exponential in the number of features.

In this paper, we propose a model-augmented  $k$ -NN method for CI testing, which simultaneously retains the computational tractability of the  $k$ -NN approach and the representational power of model-based methods. We propose a two-step approach, in which neural networks are first used to learn low-dimensional mappings of each feature; a  $k$ -NN CMI estimator is then employed on the mapped samples for CI testing.

We require two properties of our proposed mappings. (1) Subsequent CMI estimates obtained from the mappings are accurate. (2) Mapped samples share similar information about the target variable if and only if they are close in Euclidean distance. The latter property, which we refer to as *information efficiency*, captures a fundamental characteristic of the  $k$ -NN approach: local density estimates around a point are only accurate if the point is surrounded by sufficiently many similar points. The feature mappings are learned jointly by solving a single optimization problem whose objective consists of two terms, each corresponding to one of the aforementioned properties.

The main contributions of our work are as follows.

- We present an efficient Markov blanket feature selection algorithm based on the PC algorithm [Spirtes et al., 2000] (Section II).
- We show that learning a predictor of the target variable given the mappings via maximum likelihood minimizes an upper bound on the error of subsequent CMI estimates, thus satisfying property (1) above (Theorems 1 and 2).
- We propose an efficient method to perform the feature mappings for all CI tests simultaneously, by learning a single neural network using parameter sharing and a

randomization technique we call block-dropout (Section III-A).

- We propose a novel regularization technique that encourages learned feature mappings to satisfy property (2) above (Section IV).

Experiments with synthetic data are presented in Section V. As an application of our proposed approach, we consider feature selection for predicting hard disk drive (HDD) failures in Section V-C. While the HDD is the workhorse of data storage, its reliability is known to be a weak link [Elerath, 2009]. As a result, HDD failure prediction using diagnostic time-series data has drawn recent attention [Xu et al., 2016], [Lima et al., 2017], [Zhang et al., 2018]. Accurate failure prediction can reduce the amount of redundant storage needed for ensuring data reliability, thereby reducing datacenter costs. Furthermore, the results of feature selection is of interest to HDD manufacturers interested in understanding real-world failure modes.

## II. MARKOV-BLANKET FEATURE SELECTION

Consider a set of features  $\mathbf{X} = \{X_1, \dots, X_m\}$  that are used to predict a target variable  $Y$ . The goal of feature selection is to remove a maximal subset of the  $X_i$ 's that are of little or no relevance to  $Y$ . We focus on the case where  $Y$  is not high-dimensional, either initially or with the aid of dimensionality reduction. The features may be high-dimensional relative to the sample size, rendering direct application of the  $k$ -NN method impractical.

**Definition 1** (Markov blanket). A subset  $S_M \subseteq \mathbf{X}$  is a Markov blanket of  $Y$  if it is a minimal set, such that for any subset  $S \subseteq \mathbf{X}$ ,  $Y$  is independent of  $S$  conditioned on  $S_M$ . This is denoted as  $Y \perp\!\!\!\perp S | S_M$ .

Therefore, given the Markov blanket, the values of the rest of the variables become superfluous. Any approach which picks relevant features in the sense of Definition 1 is referred to as Markov blanket feature selection.

Let  $\mathcal{G}$  be the DAG, corresponding to the Bayesian network of  $\mathbf{X} \cup \{Y\}$ .  $X_i$  is called a parent of  $Y$  if there is an edge  $X_i \rightarrow Y$ , and a child of  $Y$  if there is an edge  $Y \rightarrow X_i$  in  $\mathcal{G}$ . Under some conditions (see Supplementary Materials), the Markov blanket of each variable is unique and consists of its parents, its children, and the other parents of its children (called the *coparents*) [Koller and Friedman, 2009].

In many applications, the target variable cannot be the *cause* of any of the features in the system. For instance, this is always the case when features are time series and the target is a variable to be predicted at the end of the time interval horizon. In this case, Markov blanket feature selection is equivalent to causal feature selection, desirable for its robustness to shifts in the distributions [Guyon et al., 2007]. This connection is explored in more details in Section A of the Supplementary Materials.

From Definition 1 it is evident that a single CI test is sufficient to determine whether a feature belongs to the Markov blanket of the target variable; of course, this test

---

## Algorithm 1 Markov Blanket Feature Selection

---

```

1: Initialize:  $Adj = \mathbf{X}$ ,  $CoP = \emptyset$ .
2: for  $c$  from 0 to  $\Delta$  do
3:   for  $X_i \in \mathbf{X}$  do
4:      $S_{i,c} = \{A : A \subseteq Adj \setminus \{X_i\}, |A| = c\}$ 
5:     for  $A \in S_{i,c}$  do
6:       if  $Y \perp\!\!\!\perp X_i | A$  then
7:          $Adj = Adj \setminus \{X_i\}$ 
8:       break
9:     end if
10:   end for
11: end for
12: end for
13:
14: for  $X_i \in \mathbf{X} \setminus Adj$  do
15:   if  $Y \not\perp\!\!\!\perp X_i | Adj$  then
16:      $CoP = CoP \cup \{X_i\}$ 
17:   end if
18: end for
19: return  $Adj \cup CoP$ 

```

---

is performed conditioned on all the rest of the features. In practice, evaluating conditional independencies for variables from a large alphabet requires a large number of samples. Therefore, the aforementioned naive approach leads to low accuracy when the sample size is not large.

Our feature selection approach is presented in Algorithm 1, which provides an efficient method for identifying the Markov blanket. In this algorithm,  $\Delta$  denotes the maximum degree of the underlying Bayesian network, which in practice can be treated as a hyperparameter. As in the PC algorithm for causal structure learning [Spirtes et al., 2000], for the conditioning set, we start with an empty set and gradually increase the number of variables that we condition on in Algorithm 1 (lines 3-12). As in the PC algorithm, the computational complexity of this part of the algorithm is polynomial in the number of features. This part of the algorithm outputs the set  $Adj$ , which is the set of all features which are adjacent (parent or children) to the target variable. As mentioned earlier, coparents of  $Y$  also belong to the Markov blanket of  $Y$ . Coparents have the property that they are statistically dependent conditioned on any subset of variables which contains at least one of their common children [Pearl, 2014]. Therefore, in order to find the coparents of  $Y$  we perform a CI test conditioned on variables adjacent to  $Y$  (lines 13-17). Therefore, Algorithm 1 returns the set of all adjacent and coparent variables of  $Y$ .

## III. LEARNING THE FEATURE MAPPINGS

We use CMI as the test statistic for the CI tests in Algorithm 1. For random variables  $X_1$ ,  $X_2$ , and  $Y$ , the CMI between  $X_1$  and  $Y$  given  $X_2$  is defined as

$$I(X_1; Y | X_2) = \mathbb{E}_{Y, X_1, X_2} \left[ \log \frac{dP_{X_1 Y | X_2}}{d(P_{X_1 | X_2} P_{Y | X_2})} \right], \quad (1)$$

where  $P_{X_1Y|X_2}$ ,  $P_{X_1|X_2}$ , and  $P_{Y|X_2}$  are the conditional distributions. When the conditioning on  $X_2$  is removed, (1) is known as the mutual information (MI) between  $X_1$  and  $Y$ , and is denoted by  $I(X_1; Y)$ .

As mentioned in the introduction, each feature  $X_i$  is first mapped to a low-dimensional representation denoted by  $Z_i = f_i(X_i)$ . Let  $X = [X_1 \ X_2 \ \dots \ X_m]$  and  $Z = [Z_1 \ Z_2 \ \dots \ Z_m]$ . Similarly, denote  $f(X) = [f_1(X_1) \ f_2(X_2) \ \dots \ f_m(X_m)]$  such that  $Z = f(X)$ . Algorithm 1 requires estimating a collection of CMI quantities of the form  $I(Y; X_i|S)$  for conditioning sets  $S \subseteq \mathbf{X} \setminus \{X_i\}$ . To get around the practical issues arising from  $X_i$  being high dimensional, each  $I(Y; X_i|S)$  is estimated by  $I(Y; Z_i|S')$ , such that  $S' = \{Z_i : X_i \in S\}$ . One approach to designing  $Z$  for this task is to minimize the following:

$$\min_Z |I(Y; X_i|S) - I(Y; Z_i|S')|. \quad (2)$$

Since the underlying distributions are unknown, (2) is intractable. Theorems 1 and 2 find objectives that minimize an upper bound on (2) in the  $|S| = 0$  and  $|S| = 1$  cases respectively, and Section III-A discusses the general case. In the following, let  $q_{Y|Z}$  be a parametric surrogate for the true conditional distribution  $P_{Y|Z}$ , where  $q_{Y|Z}$  could be either a discrete distribution or a probability density.

**Theorem 1.** When  $|S| = 0$ , the following minimizes an upper bound on (2):

$$\max_{Z, q_{Y|Z}} \mathbb{E}_{XY \sim P_{XY}} [\log q_{Y|Z}]. \quad (3)$$

Intuitively,  $Z$  is encouraged to be a sufficient statistic of  $X$  for  $Y$ . The following theorem shows a similar result when  $|S| = 1$ , i.e.  $S = \{X_j\}$  for some  $j \neq i$ . Let  $q_{Y|Z}$  and  $q_{Y|Z_j}$  be surrogates of  $P_{Y|Z}$  and  $P_{Y|Z_j}$  respectively.

**Theorem 2.** Let  $S = \{X_j\}$  for some  $j \neq i$ . The following minimizes an upper bound on (2):

$$\max_{Z, q_{Y|Z}, q_{Y|Z_j}} \mathbb{E}_{XY \sim P_{XY}} [\log q_{Y|Z} + \log q_{Y|Z_j}]. \quad (4)$$

Recall the discussion in Section II. When  $m = 1$ , we need to estimate up to 4 different CMIs:  $I(Y; Z_1)$ ,  $I(Y; Z_2)$ ,  $I(Y; Z_1|Z_2)$ , and  $I(Y; Z_2|Z_1)$ . In general, we need to estimate up to  $m \cdot 2^{m-1}$  quantities of the form  $I(Y; Z_i|S')$ . Therefore, Theorems 1 and 2 imply that we need to solve an exponential number of optimization problems. In the following subsection, we propose an efficient approach to circumvent the exponential computational time.

#### A. Parameter Sharing and Block-Dropout

We propose a single optimization objective for arbitrary  $m$  based on parameter sharing and a randomization technique that we call *block-dropout*.

We share two sets of parameters. First, we find a single mapping  $f$  that is used for all CMI estimations. Second, we share a single set of surrogate conditional distributions between all of the optimization problems implied by Theorems

1 and 2. In order to estimate every pairwise information-theoretic quantity involving  $Y$  and all possible conditioning sets,  $2^m - 1$  such distributions are needed. Since the mappings and surrogate distributions are all shared, we consider  $2^m - 1$  optimization subproblems. Note that the objective in (4) can be interpreted as a joint minimization over two objectives of the form (3), one given  $Z = [Z_1 \ Z_2]$  and the another given  $Z_2$ . Similarly, the  $2^m - 1$  subproblems can be enumerated by considering every conditioning set:

$$\begin{aligned} & \max \mathbb{E}[\log q_{Y|Z_1}], \\ & \max \mathbb{E}[\log q_{Y|Z_2}], \\ & \dots \\ & \max \mathbb{E}[\log q_{Y|Z_1, \dots, Z_{m-1}}], \\ & \max \mathbb{E}[\log q_{Y|Z_1, \dots, Z_m}]. \end{aligned} \quad (5)$$

When each surrogate distribution has parameters learned by a neural network, (5) implies that an exponential number of networks need to be trained. Instead of training those networks separately, we train a single network that specifies the function  $Z \mapsto g(Z)$ . For any subset of mappings  $S'$ , we parameterize  $q_{Y|S'}$  by simply removing the network connections in  $g$  corresponding to any  $Z_i \notin S'$ .

At every training iteration, connections to each input  $Z_i$  are temporarily removed with probability  $p_d$ ; we call this procedure *block-dropout*. This can be interpreted as an alternating optimization approach to minimizing (5) that randomly selects one of the subproblems at each iteration. Block-dropout is similar to dropout regularization, which was originally proposed as a computationally efficient method for model averaging in deep learning [Srivastava et al., 2014]. For example, applying dropout to the input layer of a neural network with  $k$  scalar inputs randomizes between  $2^k$  distinct networks with extensive parameter sharing during training. Unlike the original dropout, block-dropout removes entire feature representations  $Z_i$ , although the two are equivalent if  $Z_i$ 's are scalar-valued.

One may be tempted to minimize over a single surrogate  $q_{Y|Z}$  and not use block-dropout. The following example demonstrates an issue with this approach. Suppose  $X_1$  and  $X_2$  are identical copies containing the same information about  $Y$ , such that  $I(Y; X_1) = I(Y; X_2) > 0$ . Without block-dropout,  $f_1$  and  $f_2$  are not guaranteed to produce  $Z_1$  and  $Z_2$  satisfying  $I(Y; X_1) = I(Y; Z_1) = I(Y; Z_2)$ . This is due to the fact that the best predictor of  $Y$  given both  $X_1$  and  $X_2$  is no better than the best predictor of  $Y$  given  $X_1$  only. Suppose  $f_2 \equiv 0$  and  $f_1(X_1) = X_1$ ; no predictor given both  $X_1$  and  $X_2$  is strictly better than the optimal predictor given  $Z_1$  and  $Z_2$ , yet  $I(Y; Z_2) = 0$ . Note that the error in estimating  $I(Y; X_2)$  will also propagate to the estimation of  $I(Y; X_1|X_2)$ . This example demonstrates that while redundancy in the input variables need not be retained for prediction, any redundancy should be retained for CMI estimation.

The parameter sharing and block-dropout can be formalized as follows. Let  $W$  be a random vector, whose entries  $W_1, \dots, W_m$  are i.i.d. Bern( $1 - p_d$ ) random variables. Define

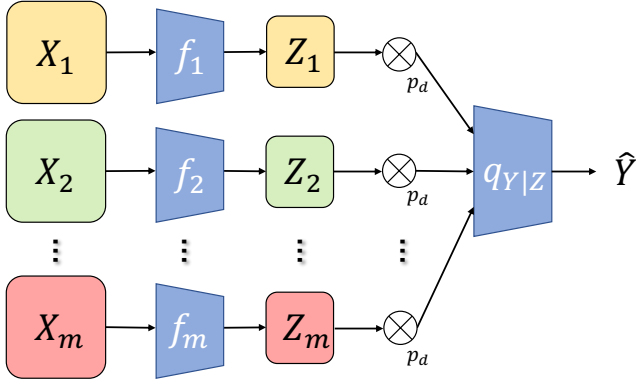


Figure 1: Proposed Model Structure.  $X_1, \dots, X_m$  are individually mapped to representations  $Z_1, \dots, Z_m$ ;  $g$  subsequently produces  $\hat{Y}$ , a prediction of  $Y$ . The symbol  $\otimes_{p_d}$  denotes the *block-dropout* operation.

$Z \bullet W := [Z_1 \cdot W_1 \quad Z_2 \cdot W_2 \quad \dots \quad Z_m \cdot W_m]$ . For function classes  $\mathcal{F}$  and distribution class  $\mathbb{Q}^g$  parametrized by neural network  $g$ , we define  $q_{Y|Z}(Y|Z \bullet W)$  as the *subset likelihood* of data under distribution  $q_{Y|Z} \in \mathbb{Q}^g$ . We perform the maximization given by

$$\max_{\substack{f \in \mathcal{F} \\ q_{Y|Z} \in \mathbb{Q}^g}} \mathbb{E}_{XYW} [\log q_{Y|Z}(Y|Z \bullet W)], \quad (6)$$

which is the expected log subset likelihood of the data under the model specified by  $g(Z \bullet W)$ . For example, minimizing the mean squared error  $\mathbb{E}[(g(Z \bullet W) - Y)^2]$  corresponds to parameterizing  $q_{Y|Z}$  as a unit-variance normal distribution with mean  $g(Z \bullet W)$ . Figure 1 illustrates the proposed model structure.

#### IV. INFORMATION EFFICIENCY

The second step of our approach employs the  $k$ -NN CMI estimator on the learned feature mappings for CI testing. We now discuss the properties of the  $k$ -NN estimator and propose a novel regularization term that is added to the subset likelihood maximization in (6) in order to improve the performance of the subsequent  $k$ -NN CMI estimation.

The  $k$ -NN estimator can be motivated as follows. A straightforward approach to estimating CMI is to discretize the data and substitute empirical probability masses into Eq. (1); this is known as the plug-in estimator. However, quantization introduces a non-negligible bias [Paninski, 2003]. The  $k$ -NN approach, based on the widely-adopted  $k$ -NN estimator of differential entropy [Kozachenko and Leonenko, 1987], was introduced as an improvement to the plug-in approach [Kraskov et al., 2004], [Frenzel and Pompe, 2007].

In this work, we consider a modification of the original  $k$ -NN approach that is consistent in the case of discrete-continuous mixtures [Gao et al., 2017]. In the continuous case, the joint density is assumed to be constant in a hypercube centered around each data point; the size of this hypercube is determined by the point's Euclidean distance to its  $k$ -nearest

neighbor. A review of the  $k$ -NN estimator is provided in the Supplementary Materials.

The  $k$ -NN estimator is consistent under mild assumptions [Gao et al., 2017], [Gao et al., 2018]. Even so, it can exhibit arbitrarily high sample complexity due to its reliance on Euclidean distance. Notably,  $k$ -NN is known to under-perform for distributions with non-global support, a phenomenon known as *boundary bias*. Intuitively, the  $k$ -NN distance for a point on the boundary shrinks more slowly than the distance for a point in the interior of the support as the sample size grows. As a result, for a fixed  $k$ , densities on the boundaries tend to be systematically under-estimated.

Boundary bias is an example of a fundamental issue with the  $k$ -NN approach: the estimation of the density at a point is not accurate unless there are sufficiently many *similar* data points around that point. Indeed, the sample complexity of the  $k$ -NN method is strongly related to the rate at which  $k$ -NN distances shrink as sample size grows; the faster  $k$ -NN distances converge to zero, the better the sample complexity [Gao et al., 2018]. We formalize this intuition by introducing the concept of information efficiency defined as follows. For this definition we use the notion of the Jeffreys divergence [Jeffreys, 1948] between two distributions  $P$  and  $Q$ , which is defined as

$$D_J(P||Q) = \frac{1}{2}D(P||Q) + \frac{1}{2}D(Q||P), \quad (7)$$

where  $D(\cdot||\cdot)$  denotes the KL-divergence.

**Definition 2** (Information Efficiency).  $X$  is *information-efficient* with respect to  $Y$  if for any  $\epsilon > 0$  there exists a  $\delta > 0$  such that for any realizations  $x$  and  $x'$  of  $X$ ,  $\|x - x'\| < \delta$  if and only if  $D_J(P_{Y|X=x}||P_{Y|X=x'}) < \epsilon$ , where  $\|\cdot\|$  is any norm on the domain of  $X$ .

The word “efficiency” is used to emphasize that Definition 2 is a condition for how efficiently the  $k$ -NN method uses the data points. Section V provides an example that shows that the sample complexity of  $k$ -NN for estimating  $I(X; Y)$  can be improved by replacing samples of  $X$  with those of  $f(X)$ , where  $f(X)$  is both information efficient and a sufficient statistic. We chose Jeffreys divergence as a distance measure between distributions because it is symmetric and can be computed analytically in many cases.

##### A. Regularization for Information Efficiency

To produce a statistic  $Z$  which exhibits the information efficiency property with respect to  $Y$ , we introduce a regularization term that correlates Euclidean distance in the  $Z$ -plane with information contained about  $Y$  in the predictor  $q_{Y|Z} \in \mathbb{Q}^g$ . In the following, we assume that  $q_{Y|Z}$  represents either a positive discrete distribution or a continuous density with shared support for all outcomes of  $Z$ . Let  $Z$  and  $\tilde{Z}$  be two independently mapped points, i.e.  $Z = f(X)$  and  $\tilde{Z} = f(\tilde{X})$  for two independent and identically drawn  $X$  and  $\tilde{X}$ . Consider the regularization term

$$R(Z, \tilde{Z}) = \left( \|Z - \tilde{Z}\|_2 - D_J(q_{Y|Z}||q_{Y|\tilde{Z}}) \right)^2. \quad (8)$$

Minimizing  $R(Z, \tilde{Z})$  simultaneously pushes dissimilar  $Z$ 's apart while pulling similar  $Z$ 's together. In order to enforce block-dropout,  $R$  is computed using samples of  $V := \mathbb{E}_W[Z] = (1 - p_d)Z$  and  $\tilde{V} := \mathbb{E}_W[\tilde{Z}] = (1 - p_d)\tilde{Z}$  instead of samples of  $Z$  and  $\tilde{Z}$ .

Adding the regularization term to the subset likelihood maximization of (6) results in the program

$$\max_{\substack{f \in \mathcal{F} \\ q_{Y|Z} \in \mathbb{Q}^g}} \mathbb{E}_{XYW} [\log q_{Y|Z}(Y|Z \bullet W)] + \lambda \mathbb{E}_{XY} [R(V, \tilde{V})], \quad (9)$$

where  $\lambda$  is a hyperparameter. The program in (9) could be solved with stochastic gradient descent (SGD), as stated in Algorithm 2.

---

**Algorithm 2** SGD Implementation of (9)

---

```

1: for number of training iterations do
2:   Obtain  $b$  samples of  $(Y, X)$ :  $\{(y^{(i)}, x^{(i)})\}_{i=1}^b$ 
3:   Obtain  $b$  samples of  $W$ :  $\{w^{(i)}\}_{i=1}^b$ 
4:   Compute  $\{z^{(i)}\}_{i=1}^b$ , where  $z^{(i)} = f(x^{(i)})$ 
5:   Shuffle  $z$  samples to obtain  $\{\tilde{z}^{(i)}\}_{i=1}^b$ 
6:   Update  $f, g$  by ascending:
7:    $\nabla_{\frac{1}{b} \sum_{i=1}^b [\log q_{Y|z^{(i)}}(y^{(i)}|z^{(i)} \bullet w^{(i)})$ 
8:      $+ \lambda \cdot R((1 - p_d) \cdot z^{(i)}, (1 - p_d) \cdot \tilde{z}^{(i)})]$ 
9: end for
```

---

## V. EXPERIMENTS

In this section, we evaluate our proposed method both on synthetic and real data.

### A. Bullseye Dataset

Consider random variables  $R \sim \text{Unif}\{[1, 2] \cup [3, 4]\}$ ,  $\Theta \sim \text{Unif}[0, 2\pi]$ , and  $N \sim \text{Unif}[-\epsilon, \epsilon]$  for  $0 \leq \epsilon \leq 0.5$ . Let  $X = (R \cos \Theta, R \sin \Theta)$  and  $Y = R + N$ . The support of  $X$ , which resembles a bullseye in  $\mathbb{R}^2$ , is plotted in Figure 2a for  $\epsilon = 0.3$ . We refer to our proposed augmented  $k$ -NN with and without the proposed regularization term in (8) as Aug-regularized and Aug-nominal, respectively. The distinction is made to illustrate the effect of the regularization (8). The learned statistic  $Z$  is 2-dimensional, and  $q_{Y|Z}$  is chosen to be a unit-variance normal with mean  $g(Z)$ .

Figures 2b and 2c illustrate the difference between the  $Z$  statistics produced by the two methods, which we denote as  $Z_{\text{nominal}}$  and  $Z_{\text{regularized}}$ . The samples are plotted over a heat map of  $g(Z)$ . Since  $g(Z)$  parameterizes the surrogate distribution, the information efficiency property requires points along constant contours of  $g$  to be close in Euclidean distance. Unlike the samples of  $Z_{\text{nominal}}$ , samples of  $Z_{\text{regularized}}$  are clustered around a single line resembling an embedding of  $R$  in  $\mathbb{R}^2$ .

**Estimation of  $I(X; Y)$ .** Note that  $X$  does not satisfy the information efficiency property with respect to  $Y$ , since any two  $X$  values with the same radial distance from the origin carry the same information about  $Y$ . Furthermore, the

geometry of the support of  $X$  introduces a boundary bias. On the other hand, the statistic  $R = \|X\|_2$  is information efficient with respect to  $Y$ , and  $I(X; Y) = I(R; Y)$ . The analytical value of this MI is derived in the Supplementary Materials. We now compare the performance of five estimators of  $I(X; Y)$ : the  $k$ -NN method using samples of  $X$  and  $R$ , (denoted by  $k$ -NN $\{X\}$  and  $k$ -NN $\{R\}$ , respectively), the model-based MINE estimator [Belghazi et al., 2018], as well as Aug-regularized and Aug-nominal. Figure 3 and 4 compares performance across values of  $\epsilon$  and sample size, respectively.

Due to the generating model of  $Y$ ,  $R$  is the optimal statistic for estimating the MI, and indeed  $k$ -NN $\{R\}$  consistently gives the best performance. Aug-regularized performs similarly to MINE, a state-of-the-art MI estimator based on neural networks. This suggests that, at least for this example, the gap in performance between  $k$ -NN and model-based estimators can be bridged using a learned information-efficient statistic. For this problem, knowledge of the joint distribution of  $X$  and  $Y$  can be used to find a statistic  $R$  that improves  $k$ -NN performance analytically. Our proposed method provides a framework for learning an appropriate statistic in the general case.

**Block-Dropout.** Let  $Y$  be the target variable and  $X$ ,  $R$ , and  $\Theta$  be features. Since  $X$  and  $R$  theoretically contain the same information, without block-dropout it is possible for the network to ignore  $X$  entirely, as explained in Section III-A. Aug-regularized is used to produce mappings of  $X$ ,  $R$ , and  $\Theta$ . Figure 5 shows estimated values of  $I(X; Y)$  for increasing levels of dropout. Even adding small amount of dropout ( $p_d = 0.1$ ) greatly reduces both the bias and variance of the resulting MI estimate.

### B. Synthetic Network Time Series

We consider random variables  $Y, X_1, \dots, X_6$  whose joint distribution satisfies the Markov and faithfulness conditions [Spirtes et al., 2000] with respect to the DAG shown in Figure 6. In this experiment, each variable is a time series.

For  $1 \leq i \leq 6$ , let  $N_i(t)$  be distributed i.i.d. according to  $\mathcal{N}(0, 1)$ , and let  $X_i(t) = 0$  for  $t < 0$ . For  $t \geq 0$ , let

$$\begin{aligned} X_4(t) &= N_4(t) \\ X_2(t) &= \frac{1}{2}X_4(t-1) + N_2(t), \\ X_1(t) &= \frac{1}{2}X_4(t-1) + N_1(t), \\ X_5(t) &= \frac{1}{\sqrt{2}}X_1(t-1) + \sqrt{0.2}N_5(t), \\ X_6(t) &= \frac{1}{\sqrt{2}}X_2(t-1) + \frac{1}{\sqrt{2}}X_5(t-1) + \sqrt{0.2}N_6(t). \end{aligned}$$

For a discrete-time random process  $H(t)$ , define  $\langle H(t) \rangle_m^+ := |\max_{t-m < k \leq t} H(k)|$  and similarly  $\langle H(t) \rangle_m^- := |\min_{t-m < k \leq t} H(k)|$ . Let  $Y(t) = \max\langle X_1(t) \rangle_m^+, \langle X_2(t) \rangle_m^- \} + N_Y(t)$ , where  $N_Y(t)$  is distributed i.i.d. according to  $\mathcal{N}(0, 0.1)$ . Finally, let  $X_3(t) = \frac{1}{\sqrt{2}}X_5(t) + \frac{1}{\sqrt{2}}Y(t) + \sqrt{0.2}N_3(t)$  for  $t \geq 0$ .

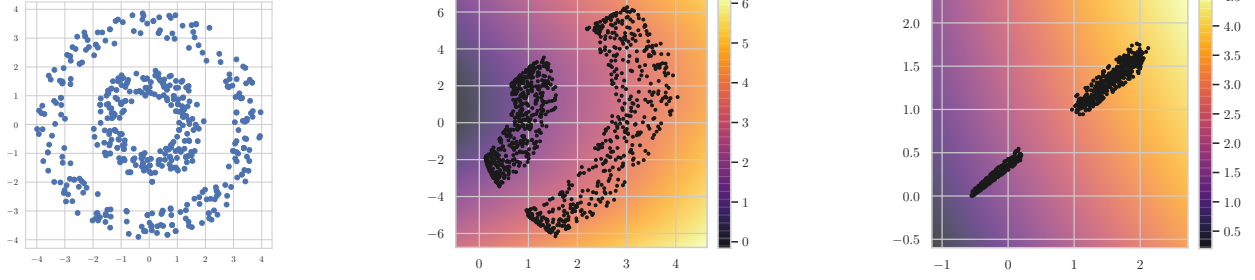


Figure 2: Bullseye dataset ( $\epsilon = 0.3$ ). (a) illustrates the support of  $X$ . Samples of  $Z$  produced by the proposed method without (b) and with (c) the proposed regularization. The heatmap depicts  $g(Z)$ .

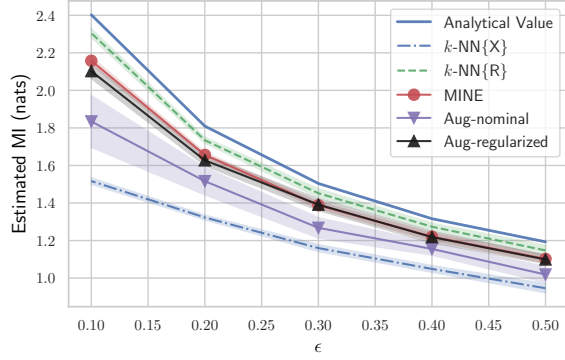


Figure 3: Performance versus  $\epsilon$ .

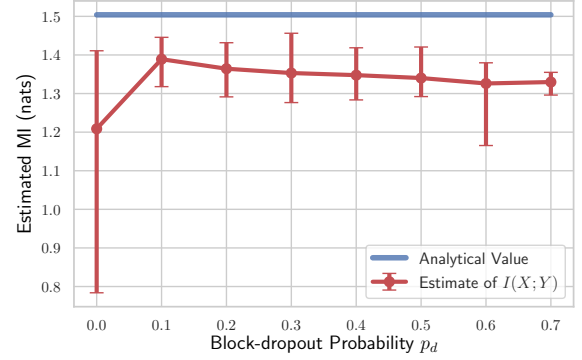


Figure 5: Performance versus  $p_d$ .

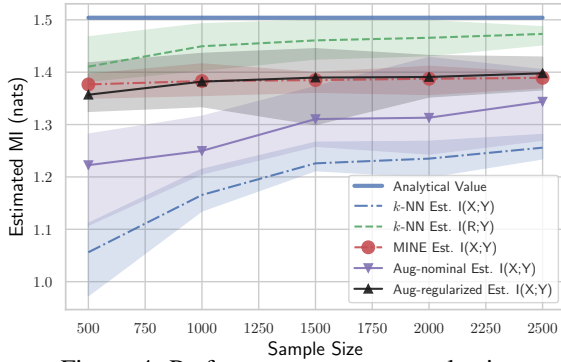


Figure 4: Performance versus sample size.

We consider vector-valued variables  $X_1, \dots, X_5$  which have entries given by  $X_1(t), \dots, X_5(t)$  respectively for  $t = 1, \dots, 15$ . The task is to identify the Markov blanket of the target variable  $Y := Y(15)$ . Testing for CI is challenging since each  $X_i$  is high-dimensional. Furthermore, the parents of  $Y$  in the DAG,  $X_1$  and  $X_2$ , are not information efficient with respect to  $Y$ . The information in  $X_1$  useful for predicting  $Y$  can be summarized by the maximum of its most recent  $m$  entries. Clearly, two realizations  $x_1$  and  $x'_1$  can satisfy  $\langle x_1(t) \rangle_m^+ = \langle x'_1(t) \rangle_m^+$ , yet  $|x_1 - x'_1| > 0$ .

We compare the performance of three different CI tests embedded in Algorithm 1 for identifying the Markov Blanket: (1) the proposed Augmented  $k$ -NN estimator, (2) the nominal  $k$ -NN estimator, and (3) the Kernel Conditional Independence Permutation Test (KCIPT) [Doran et al., 2014]. For uncondi-

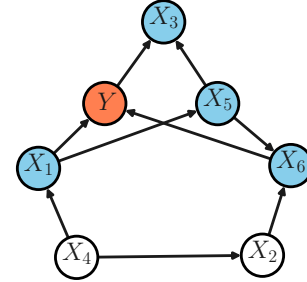


Figure 6: Graphical representation of the target variable  $Y$  and its Markov blanket.

tional independence tests, the Hilbert Schmidt Independence Criterion (HSIC) [Gretton et al., 2007] is used in place of KCIPT.

We assessed the statistical significance of the  $k$ -NN-based CI test using a non-parametric bootstrapping procedure [Diks and DeGoede, 2001]. For the unconditional independence test between  $Y$  and  $X_i$ , we randomly shuffled samples of  $X_i$ . This is carried out  $L$  times. For each  $\ell \in \{1, \dots, L\}$ , we estimated  $I(Y; X_i^\ell)$ , where  $X_i^\ell$  denotes the shuffled version of  $X_i$ . The estimated values of  $I(Y; X_i^\ell)$  are assumed to be from the null distribution ( $Y \perp\!\!\!\perp X_i$ ), and the resulting p-value is compared with a threshold (we use the common value 0.05) [Diks and DeGoede, 2001]. For CI tests, we used the nearest-neighbor permutation-based shuffling method proposed in [Runge, 2018].

For the augmented approach, we learn mappings  $Z_i \in \mathbb{R}^5$



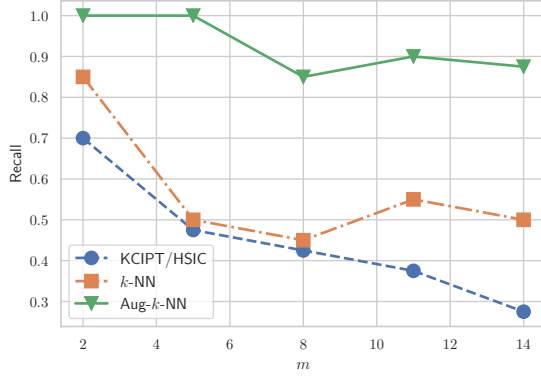


Figure 7: Recall performance of Algorithm 1 for Markov blanket identification using three CI tests.

for  $1 \leq i \leq 5$ . Since the target variable is binary, we choose  $q_{Y|Z}$  to be a Bernoulli distribution parameterized by  $g(Z)$ . Each mapping  $f_i$  is implemented by a recurrent neural network, and we use a block-dropout probability  $p_d = 0.5$ . For the  $k$ -NN step of both methods, we choose  $k = 50$ .

We evaluate the *recall* performance of Algorithm 1 with  $\Delta = 3$  using each CI test, where the recall is defined as the fraction of the true Markov blanket that was correctly identified. Figure 7 compares the recall performance of the CI tests as  $m$  is increased. Note that the recall of  $k$ -NN and KCIPT/HSIC degrade quickly as the length of time dependence is increased.

### C. Datacenter HDD Failure Prediction

Commercial and industrial HDDs report time series records of read error rate, temperature, read/write rate, and other prognostics. We used a dataset made publicly available by the Backblaze<sup>1</sup>; dataset details are provided in the Supplementary Materials. For the following experiment, we used 90-day records from 10,000 Seagate drives of a single model. 36 features, denoted as  $X_1, \dots, X_{36}$ , are reported once a day. The task is to predict a binary variable  $Y$  that indicates whether or not a drive fails at the end of the 90-day period. Around a quarter of the 10,000 drives fail.

We split the dataset into 7000 training, 1500 validation, and 1500 test samples. The training and validation samples were used to learn the mapping  $f$  as well as perform feature selection. Since the target variable is binary, we chose  $q_{Y|Z}$  to be a Bernoulli distribution parameterized by  $g(Z)$ . The mapping  $f$  was learnt using recurrent neural networks, and  $Z_i \in \mathbb{R}^3$  for  $1 \leq i \leq 36$ . We chose the block-dropout probability to be  $p_d = 0.5$ . For evaluation, two fresh predictors of  $Y$  are trained using (1) all 36 and (2) the selected time series features. Receiver operating curves (ROCs) of the two resulting models are compared using the held-out test data. Additional experimental details can be found in the Supplementary materials.

Using the proposed method, we selected the 7 features listed in Table I. Figure 8 shows that the predictor trained using

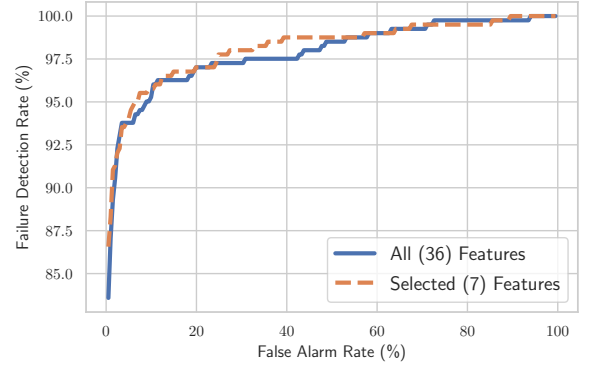


Figure 8: Receiver Operating Curves (ROC) for two predictors trained using all and selected features.

Table I: 7 Selected features for predicting HDD failures.

Current Pending Sectors	Power On Hours
Total Logical Blocks Written	Temperature
Total Logical Blocks Read	Seek Count
Load Cycle Count	

only those features performs almost identically to the predictor trained using all of the features. All of the selected features reflect measurable forms of wear. HDDs rely on a moving, mechanical actuator to read and write data from a magnetic disk. Therefore, it is expected for (logical block) read and write counts to be useful for failure prediction. Similarly, the current pending sector count is a measure of the number of memory units, or sectors, that have become unreadable. The seek and load cycle counts record how often the fragile mechanical actuator is repositioned and re-started, respectively, and are expected to be early indicators for mechanical failures. Finally, drive age and ambient operating temperatures are known to be correlated with failures [Elerath, 2009].

## VI. CONCLUSION

The need for efficient CI testing in high dimensions has limited the applicability of Markov blanket feature selection.  $k$ -NN-based CI testing methods are fast and robust, but struggle with the curse of dimensionality. On the other hand, while model-based CI testing methods have demonstrated success in high dimensions, their computational cost is prohibitive.

We proposed a novel two-step approach to performing the CI tests required by Algorithm 1 that combines the advantages of fast  $k$ -NN methods and powerful model-based methods. First, neural networks are used to map features to low-dimensional representations; a  $k$ -NN-based CMI estimator is subsequently applied to the learned feature maps for CI testing. We proposed *subset likelihood* maximization using block-dropout as a practical method for learning those feature maps. In order to improve the performance of the  $k$ -NN step in our approach, we introduced a regularization term that encourages mapped samples to be *information efficient*, i.e. share similar

<sup>1</sup>backblaze.com/b2/hard-drive-test-data.html

information about the target variable if and only if they are close in Euclidean distance. The efficacy of our proposed approach is evaluated on synthetic data as well as a real dataset of datacenter hard disk drive failures.

## APPENDIX

Let  $\mathcal{G}$  be a directed acyclic graph (DAG) in which each vertex represents one of the variables from  $\mathbf{X}$ .  $X_i$  is called a parent of  $X_j$  if we have the edge  $X_i \rightarrow X_j$ , and a child of  $X_j$  if we have the edge  $X_j \rightarrow X_i$  in  $\mathcal{G}$ . The descendants of  $X_j$  is the set of  $X_i$  such that a directed path exists from  $X_j$  to  $X_i$ . Every variable is assumed to be a descendent of itself.

**Definition 3.** For DAG  $\mathcal{G}$  and distribution  $P$  on the set of variables  $\mathbf{X}$ , the pair  $(\mathcal{G}, P)$  is called a Bayesian network if each variable in  $\mathcal{G}$  is independent of its non-descendants given its parents in  $P$  (referred to as the Markov condition). This leads to the following factorization of the joint distribution.

$$P_X = \prod_{X_j \in X} P_{X_j|Pa(X_j)},$$

where  $Pa(X_j)$  denotes the set of the parents of  $X_j$ .

Let  $\mathcal{I}(P)$  represent the set of all conditional independence relationships in  $P$ , and  $\mathcal{I}(\mathcal{G})$  represent the set of all d-separation relations<sup>2</sup> in  $\mathcal{G}$ .

**Definition 4** (Faithfulness). The distribution  $P$  is *faithful* to structure  $\mathcal{G}$  if for any two variables  $X_i, X_j$ , and any subset of variables  $X_S$ , we have

$$(X_i \text{ d-sep } X_j | X_S) \in \mathcal{I}(\mathcal{G}) \text{ if } (X_i \perp\!\!\!\perp X_j | X_S) \in \mathcal{I}(P).$$

If the Markov and faithfulness conditions hold,  $\mathcal{G}$  is called a perfect I-map for distribution  $P$ . In general, perfect I-map is not unique. For instance, for a joint distribution  $P$  on variables  $\{X_1, X_2, X_3\}$ , such that  $\mathcal{I}(P) = \{(X_1 \perp\!\!\!\perp X_3 | X_2)\}$  all three DAGs  $\mathcal{G}_1 : X_1 \rightarrow X_2 \rightarrow X_3$ ,  $\mathcal{G}_2 : X_1 \leftarrow X_2 \rightarrow X_3$ , and  $\mathcal{G}_3 : X_1 \leftarrow X_2 \leftarrow X_3$  are perfect I-maps.

**Proposition 1.** Under Markov and faithfulness assumptions, the Markov blanket of each variable is unique and consists of its parents, children, and coparents.

Causation is a topic of interest in many applied science disciplines. Knowing the causal structure among the set of variables in the system, enables us to predict the consequence of actions and interventions in the system and answer to counterfactual questions. Moreover, it provides us with a better understanding regarding the way a complex system works by explaining the interactions among the components of the system.

As mentioned in Appendix A, a Bayesian network which is an I-map for a given distribution is not unique. *Causal Bayesian network* is a Bayesian network in which directed edge  $X_i \rightarrow X_j$  implies that  $X_i$  is a direct cause of  $X_j$ . The set of direct causes (parents) of variable  $X_j$  is denoted by  $DC(X_j)$ . In the causal nomenclature, the mechanism which

takes the direct causes of a variable  $X_i$  as the input and outputs variable  $X_i$ , i.e.,  $P_{X_i|DC(X_i)}$  is called the causal module corresponding to variable  $X_i$ . According to the principle of independent causal mechanisms, if there are no latent variables in the system, the causal modules are independent of each other [Peters et al., 2017].

Knowing the causal modules enables us to perform prediction under distribution shift: Suppose in domain 1, we train a predictor for target variable  $Y$  which takes the subset of features  $X_S$  as the input. Now, if in a second domain the distribution of  $X_S$  varies, but the causal module corresponding to  $Y$  remains fixed (based on the principle of independent causal mechanisms, this is possible as the causal modules are independent), then if  $X_S$  only contains direct causes of  $Y$ , then the trained predictor can still be used in the second domain. However, if  $X_S$  also contains children of  $Y$ , as is the case for, say, a feature selection based on Markov blanket, then  $P_{Y|X_S}$  in the second domain will not necessarily remain the same as the one in the first domain. Therefore, a feature selection scheme which chooses the direct causes of the target variable, enables unsupervised domain adaptation. This scheme is referred to as *causal feature selection*.

Note that in general, performing interventions is required to identify the direct causes of the target variable, and hence, causal feature selection in general is not feasible. However, as mentioned in Section II, in many applications, the target variable cannot be the *cause* of any of the features in the system. For example, in our example of HDD failure prediction,  $Y$  represents the health state of the HDD at the end of a time interval, and as such cannot be the cause of any of the features as it cannot be the cause of past events. In this case, in the causal Bayesian network, the target variable does not have any children. Therefore, the Markov blanket of the target variable will only contain its direct causes. Hence, Markov blanket feature selection is equivalent to causal feature selection. We summarize this argument as follows:

**Assumption 1.** The target variable  $Y$  does not have any children in the causal Bayesian network.

**Theorem 3.** Under the Markov and faithfulness conditions and Assumption 1, a feature selection scheme which chooses features based on Definition 1, outputs the direct causes of the target variable.

The  $k$ -NN estimators of MI [Kraskov et al., 2004] and CMI [Frenzel and Pompe, 2007] are based on the  $k$ -NN differential entropy estimator [Kozachenko and Leonenko, 1987] proposed as an improvement over binning methods for continuous-valued random variables. We first consider the purely continuous case before using the modification proposed in [Gao et al., 2017] to handle discrete-continuous mixtures. For the following discussion, the distance  $\|\cdot\|$  denotes the  $\ell_\infty$  norm.

Consider a set of  $n$  i.i.d. samples of jointly-continuous random variables  $X, Y$ , and  $Z$ , denoted by  $\{(x^{(i)}, y^{(i)}, z^{(i)})\}_{i=1}^n$ .

<sup>2</sup>See [Pearl, 2009] for the definition of d-separation.



One approach for estimating  $I(X; Y)$  is to use the identity

$$I(X; Y) = h(Y) + h(X) - h(X, Y) \quad (10)$$

and apply the  $k$ -NN differential entropy estimator separately for each of the three terms. The idea is to average estimates of the functional  $\log p_X(x)$  around each data point  $x^{(i)}$  to obtain an estimate of the differential entropy  $h(X) = -\mathbb{E}[\log p_X(x)]$ . For the  $i$ -th data point,  $\log p_X(x^{(i)})$  is estimated by counting the number of points inside a hypercube surrounding  $x^{(i)}$ ; the side-length of this hypercube is determined by  $x^{(i)}$ 's distance to its  $k$ 'th nearest neighbor.

The contribution of Kraskov et al. was to correlate the hypercube side-lengths used between the three estimates [Kraskov et al., 2004] instead of performing the three entropy estimates separately. Their estimator has been shown to be a significant improvement both in practice and theoretically [Kraskov et al., 2004], [Gao et al., 2017]. Let  $\epsilon_k^{(i)}$  be the distance between the  $i$ -th datapoint  $(x^{(i)}, y^{(i)})$  and its  $k$ -th nearest neighbor. Define  $n_x^{(i)} := \sum_{j=1}^n \mathbf{1}\{\|x^{(i)} - x^{(j)}\|_\infty \leq \epsilon_k^{(i)}\}$  to be the number of points in the  $X$ -plane within  $\epsilon_k^{(i)}$  of  $x^{(i)}$ ;  $n_y$  is defined analogously. Let  $\psi(\cdot)$  denote the digamma function (e.g. [Abramowitz and Stegun, 1965]). For a fixed  $k$ , the MI estimator proposed by Kraskov et al. is given by  $\hat{I}_k(X; Y) = \frac{1}{n} \sum_{i=1}^n \hat{l}_{xy,k}^{(i)}$ , where

$$\hat{l}_{xy,k}^{(i)} = \log(n) + \psi(k) - \psi(n_x^{(i)}) - \psi(n_y^{(i)}). \quad (11)$$

The same idea can be used to develop a CMI estimator by making use of the identity

$$I(X; Y|Z) = h(X, Z) + h(Y, Z) - h(X, Y, Z) - h(Z). \quad (12)$$

Defining  $n_z$ ,  $n_{xz}$ , and  $n_{yz}$  analogously to  $n_x$ , the CMI estimator proposed in [Frenzel and Pompe, 2007] is given by  $\hat{I}_k(X; Y|Z) = \frac{1}{n} \sum_{i=1}^n \hat{l}_{xyz,k}^{(i)}$ , where

$$\hat{l}_{xyz,k}^{(i)} = \psi(k) + \psi(n_z^{(i)}) - \psi(n_{xz}^{(i)}) - \psi(n_{yz}^{(i)}). \quad (13)$$

We now consider the case where  $X$ ,  $Y$ , and  $Z$  are mixtures of discrete and continuous random variables. MI and CMI are well-defined in terms of the Radon-Nikodym derivative, but cannot be expressed as a function of entropies or differential entropies since the joint density is not well-defined. Therefore, the estimators in (11) and (13) are no longer consistent.

The authors of [Gao et al., 2017] propose a modification of the  $k$ -NN approach that directly estimates the Radon-Nikodym derivative in Eq. (1). The idea is to replace Eqns. (11) and (13) with an estimator that considers three cases:

- When the  $k$ -NN distance  $\epsilon_k^{(i)}$  is zero, the  $i$ -th data point is declared to be in a discrete component. In this case, a plug-in estimate of the Radon-Nikodym derivative can be used for  $\hat{l}_{xy,k}^{(i)}$  (resp.  $\hat{l}_{xyz,k}^{(i)}$ ).
- When  $\epsilon_k^{(i)} > 0$ , the  $i$ -th data point may be in a purely continuous or mixed component. It was shown in [Gao et al., 2018] that the continuous  $k$ -NN estimator is applicable for both cases, i.e.  $\hat{l}_{xy,k}^{(i)}$  is given by Eq. (11) (resp.  $\hat{l}_{xyz,k}^{(i)}$  is given by (13)).

We now summarize the mixed- $k$ -NN approach. Denote by  $\rho_{xy,k}^{(i)}$  the  $k$ -th smallest distance among  $\{d_{ij} := \max\{\|x^{(i)} - x^{(j)}\|, \|y^{(i)} - y^{(j)}\|\} : j \neq i\}$  ( $\rho_{xyz,k}^{(i)}$  is defined analogously). Let  $\tilde{k}^{(i)}$  be the number of samples such that  $d_{ij} = 0$  if  $\rho_{xy,k}^{(i)}$  (resp.  $\rho_{xyz,k}^{(i)}$ ) were 0 (discrete case), and  $k$  otherwise. The mixed-case  $k$ -NN estimators of MI and CMI are given by  $\tilde{I}_k(X; Y) = \frac{1}{n} \sum_{i=1}^n \tilde{l}_{xy,k}^{(i)}$  and  $\tilde{I}_k(X; Y|Z) = \frac{1}{n} \sum_{i=1}^n \tilde{l}_{xyz,k}^{(i)}$ , where

$$\tilde{l}_{xy,k}^{(i)} = \log(n) + \psi(\tilde{k}^{(i)}) - \psi(n_x^{(i)}) - \psi(n_y^{(i)}), \quad (14)$$

$$\tilde{l}_{xyz,k}^{(i)} = \psi(\tilde{k}^{(i)}) + \psi(n_z^{(i)}) - \psi(n_{xz}^{(i)}) - \psi(n_{yz}^{(i)}). \quad (15)$$

Alternative modifications for the mixed case include discretization and the plug-in approach and the addition of low-amplitude noise to remove discrete components. However, the superiority of the mixed- $k$ -NN approach over those alternatives has been demonstrated experimentally [Gao et al., 2017].

*Proof of Theorem 1.* The non-negativity of  $I(Y; X) - I(Y; Z)$  follows from the data processing inequality (see, e.g., [Cover and Thomas, 2006]). Since  $I(Y; X)$  does not depend on  $f$  or  $q_{Y|Z}$ , we use the following lower bound on  $I(Y; Z)$ :

$$\begin{aligned} I(Y; Z) &= \mathbb{E}_{X,Y \sim P_{XY}} \left[ \log \frac{dP_{Y|f(X)}}{dP_Y} \right] \\ &\stackrel{(a)}{=} \mathbb{E}_{X,Y \sim P_{XY}} \left[ \log \frac{dQ_{Y|f(X)}}{dP_Y} + \log \frac{dP_{Y|f(X)}}{dQ_{Y|f(X)}} \right] \\ &\stackrel{(b)}{\geq} \mathbb{E}_{X,Y \sim P_{XY}} \left[ \log \frac{dQ_{Y|f(X)}}{dP_Y} \right] \\ &\geq \mathbb{E}_{X,Y \sim P_{XY}} \left[ \log q_{Y|f(X)} \right]. \end{aligned} \quad (16)$$

The introduction of  $q_{Y|Z}$  in (a) is admissible since  $P_{Y|Z}$  is assumed to be absolutely continuous with respect to  $q_{Y|Z}$ . Furthermore, the inequality (b) follows from the fact that  $\mathbb{E}_{X,Y \sim P_{XY}} \left[ \log \frac{dQ_{Y|f(X)}}{dP_{Y|f(X)}} \right] = D(P_{Y|f(X)} \| q_{Y|f(X)})$  is non-negative and finite. Note that the right hand side of (16) is finite due to the absolute continuity of  $P_{Y|Z}$  with respect to  $q_{Y|Z}$ . Finally, maximization of the right hand side of (16) is equivalent to the desired result.  $\square$

*Proof of Theorem 2.* The chain rule of mutual information gives the following:

$$I(Y; X_1|X_2) = I(Y; X_1, X_2) - I(Y; X_2), \quad (17)$$

$$I(Y; Z_1|Z_2) = I(Y; Z_1, Z_2) - I(Y; Z_2). \quad (18)$$

Subtracting (18) from (17) and applying the triangle inequality gives

$$\begin{aligned} &|I(Y; X_1|X_2) - I(Y; Z_1|Z_2)| \\ &\leq |(I(Y; X_1, X_2) - I(Y; Z_1, Z_2))| \\ &\quad + |I(Y; X_2) - I(Y; Z_2)| \end{aligned} \quad (19)$$

By the data-processing inequality, each of the two terms on the right hand side are non-negative. Applying the result of

Theorem 1 to each term separately results in a minimization of an upper bound on the right hand side of (19).  $\square$

The ground truth MI values for the Bullseye problem are derived here. Assume that  $\epsilon \leq 0.5$ .

$$I(X; Y) = I(R; Y) \quad (20)$$

$$= h(Y) - h(Y|R) \quad (21)$$

$$= h(Y) - h(R + N|R) \quad (22)$$

$$= h(Y) - h(N) \quad (23)$$

$$(24)$$

Since  $N \sim \text{Unif}[-\epsilon, \epsilon]$ , it has differential entropy  $h(N) = \log(2\epsilon)$ . To find  $h(Y)$ , first note that  $Y$  can be seen as a randomization between the inner and outer rings:

$$Y = \begin{cases} Y_1 & \text{w.p. } 1/2 \\ Y_2 & \text{w.p. } 1/2. \end{cases} \quad (25)$$

Define  $Y_1 = R_1 + N_1$  and  $Y_2 = R_2 + N_2$ .  $R_1 \sim \text{Unif}[0.25, 0.5]$ ,  $R_2 \sim \text{Unif}[0.75, 1.0]$ , and  $N_1$  and  $N_2$  are identically distributed copies of  $N$ . The marginal distribution  $p(y_1)$  is given by

$$p(y_1) = \int_{-\epsilon}^{\epsilon} p(N = n) p(y_1|n) dn \quad (26)$$

$$= \frac{1}{2\epsilon} \int_{-\epsilon}^{\epsilon} p(R_1 = y_1 - n) dn \quad (27)$$

$$= \frac{2}{\epsilon} \int_{-\epsilon}^{\epsilon} \mathbf{1}\{y_1 \in [0.25 + n, 0.5 + n]\} dn. \quad (28)$$

There are three cases, depending on the value of  $y_1$ . Taking the integral in each case gives

$$p(y_1) = \begin{cases} \frac{y_1 - 0.25 + \epsilon}{0.5\epsilon} & \text{if } y_1 \in [0.25 - \epsilon, 0.25 + \epsilon] \\ 4 & \text{if } y_1 \in [0.25 + \epsilon, 0.5 - \epsilon] \\ \frac{0.50 + \epsilon - y_1}{0.5\epsilon} & \text{if } y_1 \in [0.50 - \epsilon, 0.50 + \epsilon] \end{cases} \quad (29)$$

The marginal  $p(y_2)$  can be obtained by shifting  $p(y_1)$ .  $h(Y)$  can now be computed numerically for different values of  $\epsilon$  using Eq. (29) and the fact that

$$h(Y) = - \int_{-\infty}^{\infty} \frac{1}{2} p(y_1) \log \left( \frac{1}{2} p(y_1) \right) dy_1 - \int_{-\infty}^{\infty} \frac{1}{2} p(y_2) \log \left( \frac{1}{2} p(y_2) \right) dy_2. \quad (30)$$

The mappings used by the Aug-nominal and Aug-regularized methods were learnt using three-layer feedforward neural networks. The predictor  $g$  was also implemented by a three-layer network; we chose  $\lambda = 0.1$  for the regularization coefficient in (8). We used  $k = 5$  for all  $k$ -NN estimators.

Recurrent neural networks were used to implement each mapping for the network time series example. The predictor function  $g$  was implemented by a three-layer network. We chose  $p_d = 0.2$  and  $\lambda = 1e-2$ . We used a sample size of 500 to test Algorithm 1. Following the recommendation in [Runge, 2018], we choose  $k = 50$  for the  $k$ -NN method, and compute

Table II: SMART Attributes for Seagate’s drive model ST4000DM000. \* denotes attributes reported in both normalized and raw form. † have only normalized values, and ‡ only raw values. There are 36 attributes in total.

*Read Error Rate	*Power On Hours
*Temperature	*Start/Stop Count
*Airflow Temperature	*High Fly Writes
*Reallocated Sectors	†Spin Up Time
*SATA Downshift Errors	†Seek Errors
*End to End Errors	†Seek Count
*Load Cycles	‡Power Off Retracts
*Command Timeouts	‡Power Cycles
*Current Pending Sectors	‡Head Flying Hours
*Reported Uncorr. Errors	‡Blocks Written
†Offline Uncorr. Sectors	‡Blocks Read
‡Cyclic Red. Check Errors	

p-values using 1000 bootstrap samples. KCIPT was configured based on the recommendations in [Doran et al., 2014].

CI testing was carried out similarly for the HDD feature selection problem. Since the sample size is larger for this dataset, we used  $k = 100$  for the  $k$ -NN methods. Each feature mapping was implemented using a two-layer recurrent neural network (RNN) followed by a linear layer; we chose each  $Z_i$  to be 3-dimensional. A three-layer feedforward network was used to implement the predictor function  $g$ . For the regularization term, we used  $\lambda = 0.02$ .

We used data collected from 10,000 Seagate ST4000DM000 HDDs. Table II lists the time-series features reported by each drive. The features are known as Self-Monitoring, Analysis, and Reporting Technology (SMART) attributes. Some of the features are reported in two separate formats: *raw* and *normalized*. The raw features can be considered as raw sensor measurements, whereas the normalized features are quantized and scaled in a manufacturer-specific way in order to be compared between HDD makes and models. Table I lists all of the features used for this experiment.

Finally, note that Seek Errors and Seek Count are not typically-reported SMART attributes. These were generated by extracting the top 16 and bottom 32 bits of the raw SMART attribute “Seek Error Rate.” Since we noticed that the normalized version of “Seek Error Rate” could be well-approximated by dividing the Seek Error count by the Seek Count, we do not use Seek Error Rates for our experiments.

## REFERENCES

- [Abramowitz and Stegun, 1965] Abramowitz, M. and Stegun, I. A., editors (1965). *Handbook of Mathematical Functions with Formulas, Graphs and Mathematical Tables*. Dover Publications, Inc.
- [Aliferis et al., 2010] Aliferis, C. F., Statnikov, A., Tsamardinos, I., Mani, S., and Koutsoukos, X. D. (2010). Local causal and markov blanket induction for causal discovery and feature selection for classification part i: Algorithms and empirical evaluation. *Journal of Machine Learning Research*, 11(Jan):171–234.
- [Belghazi et al., 2018] Belghazi, M. I., Baratin, A., Rajeshwar, S., Ozair, S., Bengio, Y., Courville, A., and Hjelm, D. (2018). Mutual information

- neural estimation. In *Proceedings of the 35th International Conference on Machine Learning*, volume 80, pages 531–540.
- [Cover and Thomas, 2006] Cover, T. M. and Thomas, J. A. (2006). *Elements of Information Theory (Wiley Series in Telecommunications and Signal Processing)*. Wiley-Interscience.
- [Diks and DeGoede, 2001] Diks, C. and DeGoede, J. (2001). A general nonparametric bootstrap test for granger causality. In *Global Analysis of Dynamical Systems*, chapter 16, pages 391–403. London: Institute of Physics.
- [Doran et al., 2014] Doran, G., Muandet, K., Zhang, K., and Schölkopf, B. (2014). A permutation-based kernel conditional independence test. In *Proceedings of the Thirtieth Conference on Uncertainty in Artificial Intelligence, UAI’14*, pages 132–141. AUAI Press.
- [Elerath, 2009] Elerath, J. G. (2009). Hard-disk drives: The good, the bad, and the ugly. *Communications of the ACM*, 52:38–45.
- [Frenzel and Pompe, 2007] Frenzel, S. and Pompe, B. (2007). Partial mutual information for coupling analysis of multivariate time series. *Physical Review Letters*, 99(20):204101.
- [Fukumizu et al., 2004] Fukumizu, K., Bach, F. R., and Jordan, M. I. (2004). Dimensionality reduction for supervised learning with reproducing kernel hilbert spaces. *J. Mach. Learn. Res.*, 5:73–99.
- [Gao et al., 2017] Gao, W., Kannan, S., Oh, S., and Viswanath, P. (2017). Estimating mutual information for discrete-continuous mixtures. In *Advances in Neural Information Processing Systems*, pages 5988–5999.
- [Gao et al., 2018] Gao, W., Oh, S., and Viswanath, P. (2018). Demystifying fixed k-nearest neighbor information estimators. *IEEE Transactions on Information Theory*, 64(8):5629–5661.
- [Gretton et al., 2007] Gretton, A., Fukumizu, K., Teo, C. H., Song, L., Schölkopf, B., and Smola, A. J. (2007). A kernel statistical test of independence. In *Proceedings of the 20th International Conference on Neural Information Processing Systems, NIPS’07*, pages 585–592.
- [Guyon et al., 2007] Guyon, I., Aliferis, C., et al. (2007). Causal feature selection. In *Computational methods of feature selection*, pages 79–102. Chapman and Hall/CRC.
- [Jeffreys, 1948] Jeffreys, H. (1948). *Theory of probability*. Oxford University Press, 2 edition.
- [Koller and Friedman, 2009] Koller, D. and Friedman, N. (2009). *Probabilistic graphical models: principles and techniques*. MIT press.
- [Kozachenko and Leonenko, 1987] Kozachenko, L. and Leonenko, N. (1987). Sample estimate of the entropy of a random vector. *Problemy Peredachi Informatsii*, 23(2):9–16.
- [Kraskov et al., 2004] Kraskov, A., Stögbauer, H., and Grassberger, P. (2004). Estimating mutual information. *Physical Review E*, 69(6):066138.
- [Lima et al., 2017] Lima, F. D. S., Amaral, G. M. R., Leite, L. G. M., Gomes, J. P. P., and Machado, J. C. (2017). Predicting failures in hard drives with lstm networks. In *Brazilian Conference on Intelligent Systems*.
- [Paninski, 2003] Paninski, L. (2003). Estimation of entropy and mutual information. *Neural computation*, 15(6):1191–1253.
- [Pearl, 2009] Pearl, J. (2009). *Causality*. Cambridge university press.
- [Pearl, 2014] Pearl, J. (2014). *Probabilistic reasoning in intelligent systems: networks of plausible inference*. Elsevier.
- [Peters et al., 2017] Peters, J., Janzing, D., and Schölkopf, B. (2017). *Elements of causal inference: foundations and learning algorithms*. MIT press.
- [Runge, 2018] Runge, J. (2018). Conditional independence testing based on a nearest-neighbor estimator of conditional mutual information. In *21st International Conference on Artificial Intelligence and Statistics (AISTATS)*, volume 84 of *Proceedings of Machine Learning Research*.
- [Sen et al., 2017] Sen, R., Suresh, A. T., Shanmugam, K., Dimakis, A. G., and Shakkottai, S. (2017). Model-powered conditional independence test. In *Proceedings of the 31st International Conference on Neural Information Processing Systems, NIPS’17*.
- [Spirites et al., 2000] Spirites, P., Glymour, C. N., Scheines, R., Heckerman, D., Meek, C., Cooper, G., and Richardson, T. (2000). *Causation, prediction, and search*. MIT press.
- [Srivastava et al., 2014] Srivastava, N., Hinton, G., Krizhevsky, A., Sutskever, I., and Salakhutdinov, R. (2014). Dropout: A simple way to prevent neural networks from overfitting. *J. Mach. Learn. Res.*, 15(1):1929–1958.
- [Xu et al., 2016] Xu, C., Wang, G., Liu, X., Guo, D., and Liu, T.-Y. (2016). Health status assessment and failure prediction for hard drives with recurrent neural networks. *IEEE Transactions on Computers*, 65(11):3502–3508.
- [Zhang et al., 2018] Zhang, J., Wang, J., He, L., Li, Z., and Yu, P. S. (2018). Layerwise perturbation-based adversarial training for hard drive health degree prediction. In *IEEE International Conference on Data Mining*.